Part I: Frequency Offset Acquisition and Tracking Algorithms

Mohamed K. Nezami
Mnemonics Inc.
3900 Dow Rd, Melbourne, FL 32934

I. Introduction

Wireless receivers process signals that bear information as well as disturbances caused by the transmitter/receiver circuits and channel impairments such as fad:ing, interference, and additive white gaussian noise (AWGN). Usually, the receiver knows only some statistical properties of the signal and disturbances. From these statistical properties and using a finite observation of the received signal, the receiver is able to estimate the transmitted data symbols. The receiver makes the decision on the received data using locally generated symbol clock and carrier oscillator, both of which are not referenced to the actual versions used to generate the data at the transmitter. The receiver has to estimate the offset between locally generated carrier and symbol clock to those used at the transmitter. Clock mismatches are labeled as time jitters, while local carrier mismatches are labeled either as phase rotation errors or frequency offset errors. Carrier phase recovery is the process known as carrier tracking, where the receiver estimates the offset between the local oscillator phase and the actual phase of the transmitted carrier. Carrier frequency offset recovery is known as carrier acquisition, and it is the process of estimating the offset between the frequency drift/change of the local oscillator and the actual (received) carrier frequency transmitted at the transmitter. The methods in which the receiver estimates carrier mismatches can be feed forward (open Loops) or feedback (closed loops) synchronization. Feed forward method is characterized by the absence of hang up and cycles slips, and fast and accurate acquisition. Such advantages are absent with conventional feedback synchronizers such as Costas loop. Another advantage of feed forward algorithms is that the synchronizer can be fully implemented using digital signal processing techniques as shown in figure 1.

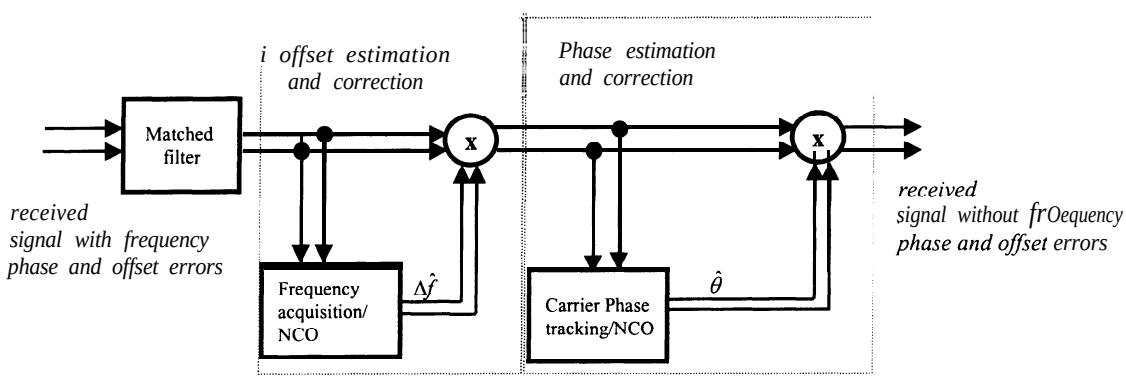

Figure 1: Complete Feed Forward Baseband synchronization system

This paper reports an overview of existing as well as presenting new carrier acquisition and tracking systems that are used in modem satellite and personal communication receivers. In particular algorithms that acquire and track the carrier frequency in the absence of symbol timing or a data preamble sequence. The objective is to investigate

these algorithms. Then verify their applicability and performance in realistic situations such as wireless hand held cellular and satellite TDMA receivers. The performance evaluation of the algorithms is conducted through simulations and theoretical analysis. The work is performed in two parts. In the first part; we report the mathematical development of these algorithms and their statistical properties and "pull in" range in AWGN channels. In the second part, we present the performance analysis of the recovery process through computer simulation for a variety of applications concerning satellite communications receivers, in particular, techniques proposed that acquires carrier offsets when the initial error (offset) is too large to employ conventional loops (open loops or closed loops). Furthermore, we present a practical means of implementing these algorithms using commercial digital signal processor chips.

II. Carrier Frequency Acquisition and Tracking

In addition to removing carrier frequency offsets, phase errors between the received signal and the local oscillator has to be removed as well. Phase error can result in rotation of the received symbols resulting in degradation of the bit error rate and ultimately degradation in the receiver sensitivity. The BER deterioration as a result of phase mismatches is defined as being the amount of increase in signal power (in dB) that is needed in order to get the same BER performance from a receiver that uses an ideal carrier synchronizer [1,2,3,4,5,6,7,8,9], and given by (1)

$$D = 4.3(1+ E, /N\&T; \quad [dB] \qquad (1)$$

where E, $/N_o$ is the symbol energy to noise ratio, $\%^2$ is the phase variance of the estimated phase out of the synchronizer. For second order Costas loop, the phase variance is given by (2)

$$\%^2 = s \quad F a d^2 1 \qquad (2)$$

where *B,* is the one sided loop bandwidth, and *T* is the symbol rate (loop iteration rate). Acquiring and tracking carriers using Costas loops for short-burst satellite TDMA signals can prove to be a difficult task. The loop acquisition time as a function of loop bandwidth and the frequency offset to be acquired [6] is given by (3)

$$t_{acq} = \frac{n^2(2xAf)'}{16<(2\sim B,)\sim} + \frac{27\sim}{2nrB,} - becl \qquad (3)$$

Where< is the second order type loop damping factor and Af is the frequency offset. To achieve faster acquisition, the loop bandwidth in equation 3 has to be increased, while doing so, the phase error variance increases in equation 2, leading to reduction of BER in equation 1. The term on the right-hand side of equation 3 is the tracking time [6], while the term on the left-hand side is the "pull-in" or acquisition time. To demonstrate the loop bandwidth, acquisition timing and BER degradation, let us assume a frequency offset due to Doppler as 1 kHz and a < = 0.707, figure 2 shows a plot of t,, , phase variance and BER degradation as a function of loop bandwidth *B,*. Clearly as the loop becomes

narrower to achieve lower BER degradation by having lower ol, the acquisition time becomes impractical for typical short TDMA satellite bursts [S]. Meanwhile, if the loop bandwidth is widened to achieve faster acquisition, both phase variance and BER deterioration become large. Ideally and based on our lab experience, a typical Costas loop bandwidth of 25-50 Hz is required for satellite modems with d.ata rates of less than 56 kbps using MPSK. This allows for a maximum phase variance of 10^{m3} rad^2 (or a standard deviation of g_B =I.8 lOS^o), which results in a BER degradation less than 0.1 dB. One way to speed up feedback loops is by utilizing frequency sweep or variable loop bandwidth, both of which are complex to utilize and may result in destabilizing the loop operation. Loops with a variable loop bandwidth have been utilized [121, however their implementation creates a multiple magnitude of implementation problems, and needs continued maintenance. DFT aided loops have also been used, however a large number of DFT bins (high resolution) is required to estimate the carrier to an offset less than 10 Hz [81, such resolution requires huge computational resource and have rendered useless for mobile low power receivers.

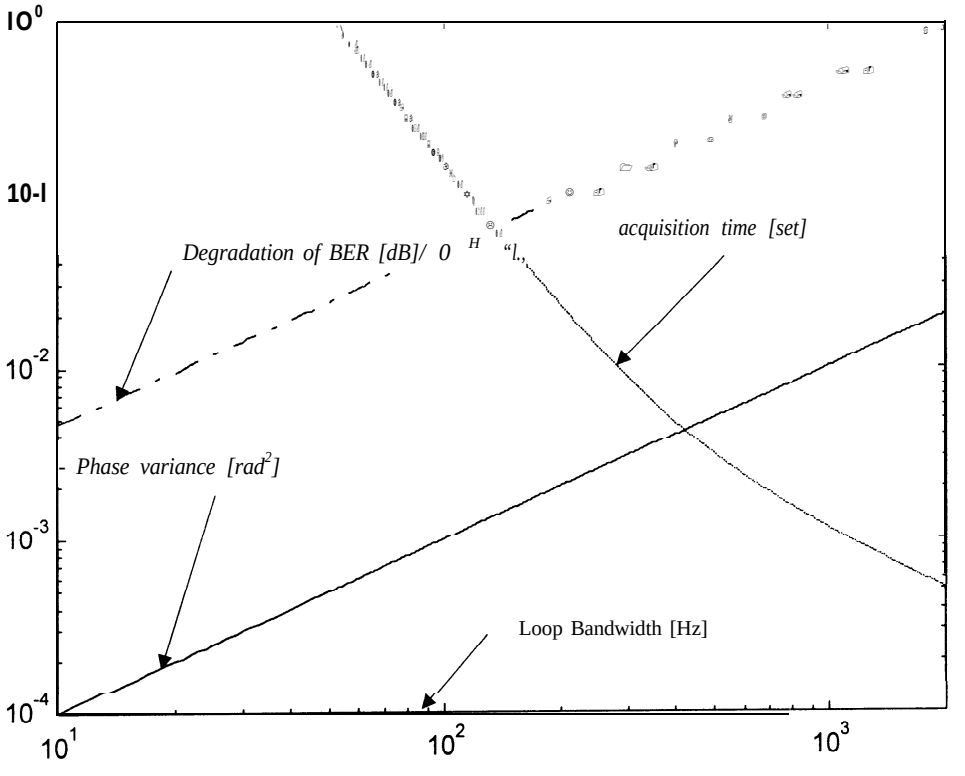

Figure 2: Loop bandwidth versus carrier phase variance and BER deterioration for Feedback type carrier recovery systems.

11.1 Open Loop M^fh Power Frequency Acquisition Algorithm

To derive the mathematical representation of this algorithm, we start by representing the received matched filter complex M-PSK baseband signal in AWGN n(t) by

$$z(t) = e^{j(2\pi\Delta ft+\theta(t)+\phi(t))} + n(t) \qquad (4)$$

where 4(t) is the phase due to the transmitted symbols, e(t) is the phase term that includes the carrier phase error and phase rotation introduced by the propagation channel, which may vary in time, however for most of our analysis its assumed to vary slow when compared to the variation in phase due to symbols, Af is the frequency offset introduced by either channel effects, or offset errors due to the various up and down conversions that the signal encounters while being transmitted and received. To perform frequency offset detection, we pass the matched filter signal through a differential digital detector which eliminates the carrier phase error rotation, by *z(kT)z** ((k - *N)T)* , this yields a signal that contains frequency error offsets given by (5)

$$\begin{aligned} & z(kT)z^* ((k - N)T) = \exp G(2nfkT \\ & - 2niq((k - N)T) + B(kT) \\ & - B((k - N)T) + @(kT) \\ & - 4((k - NY?) + n'(kW \end{aligned} \qquad 0$$

where *k* is the index of the baseband samples, n'(t) is a complex AWGN with real and imaginary parts that are independent and have a variance of a,' = [2E, / N_O]-' , or $4 = T[T_s\ 2E, I\ N_o]$-', whereT$_s$ is the sample time. The differential phase detection causes cancellation of *B(t)* , because such phase variation is assumed to be equal between two consecutive symbols, so the component $e^{j(B(kT)-B((k-N)T))}$ im (5) yields a unity term. For simplicity we will lump the frequency offset terms due to offset difference between N consecutive samples as being $e^{j(2nwT-2nAf((k-N)T))} = ej(2WW$ (notice that we assume N=l or one symbol period unless otherwise indicated, or the over-sampling factor, such as denoting every 4th sample is a symbol period). The term e IS due to symbol modulations, this term can be removed by processing the signal through an M-power non-linearity, where the value A4 is an integer equal to the modulation symmetry angle (i.e., for QPSK M=4, for BPSK M=2). QPSK modulation is removed due to the fact that $e^{4j(i7fn)} = 1$, *for n=O,1,.2,3* . . . . Doing so yields a noisy sine-wave signal in equation 5 with a fundamental frequency that is equal to the frequency offset associated with the received baseband signal. For QPSK, where M=4, this is given by (6)

$$Yk = e4j(2GtT) + n'(kT) \qquad (6)$$

Designating the k^{th} complex sample of the differential baseband signal as being a real part Re(z,) = I, and an imaginary part Im(z,) = Q_k , making the current matched filter sample z, = I, + jQ_k , and the previous sample, which is N-samples back in time is z*M = I,+ - je,-, . Substituting both terms into (5) yields (7)

$$\text{ZkZk-,ji} = \underbrace{[I_k I_{k-N} + Q\&-N]+}_{R\&;-N\ 3} \cdot \&\ \underbrace{dlr-,v - Qk-iv\&\ 1}_{Im(li_v)} \qquad (7)$$

Equation 7 represents a frequency-offset detector. It can be shown that

LA + jQk-NQk = cos(27~MAfl) and QklkVN - jQ,-, *I,* = sin(2xMAfl)

Both terms are commonly referred to as being the dot and cross product terms, respectively. Expanding both terms further yields an initial frequency acquisition value given by (8)

$$2nMAfl = \arg\{(zkzi-N)M \qquad (8)$$

where arg{x) = tan-' (x) . In order to reduce random variations of (8) due to AWGN and phase residuals from data modulations, equation 8 is averaged over L-symbols yielding a final carrier offset estimator algorithm represented by (9)

$$\Delta\hat{f} = \frac{R_s}{2\pi M}\tan^{-1}\left\{\frac{\sum_{k=1}^{L}\mathrm{Im}\left[(z_k z_{k-N}^{*})^{M}\right]}{\sum_{k=1}^{L}\mathrm{Re}\left[(z_k z_{k-N}^{*})^{M}\right]}\right\} \quad [\mathrm{Hz}] \qquad (9)$$

This algorithm has a maximum capture range of Af 5 + *R,* /2M Hz, or roughly 10% of the transmitted data rate, where $R, = l/T$. For instance, using a 10 ksps symbol rate satellite modem, and a QPSK modulated signal (A4=4), the upper limit of this algorithm is Af= +2500 Hz as shown in figure 3. The algorithm's estimate accuracy as a function of variable SNR is shown in figure 4 for detecting a 1 kHz offset. Clearly the algorithm's performance is v^{e}ry accurate for SNR greater than 10 dB.

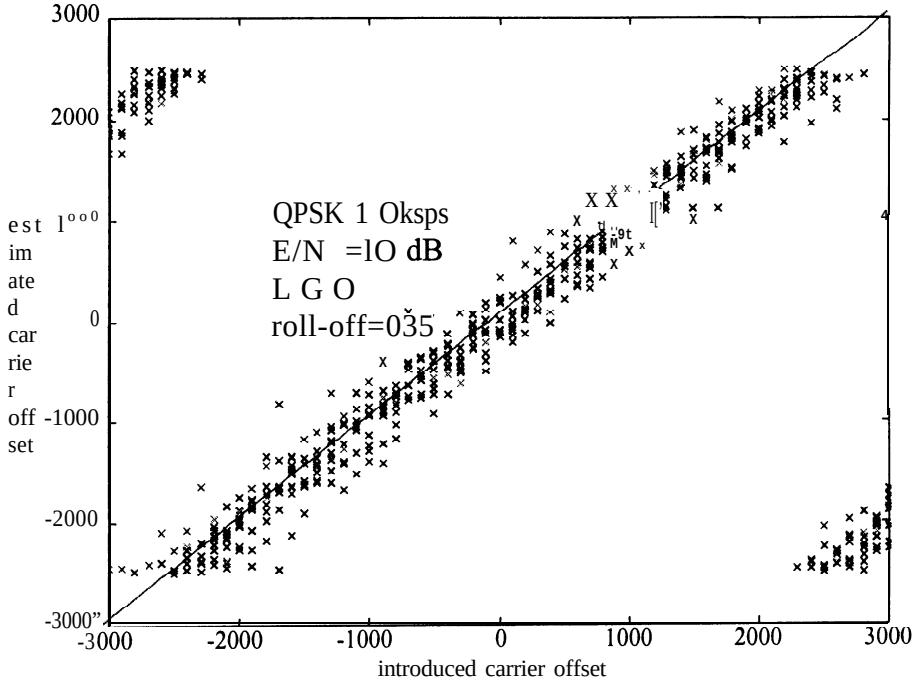

Figure 3: M[th] power carrier frequency estimator range performance

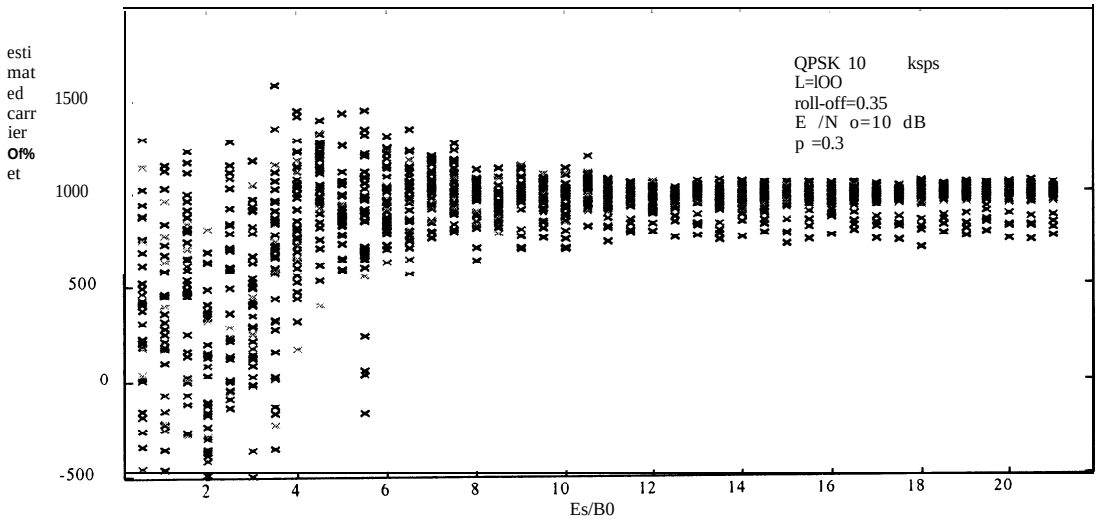

Figure 4: M[th] power carrier offset estimator performance for an offset of 1kHz

After frequency offset correction, the matched filter signal still has an arbitrary phase error that have to be estimated and compensated. Before we introduce the phase estimation stage, it is of interest to present several other frequencies offset algorithms that differ from (9) in term of implementation and performance.

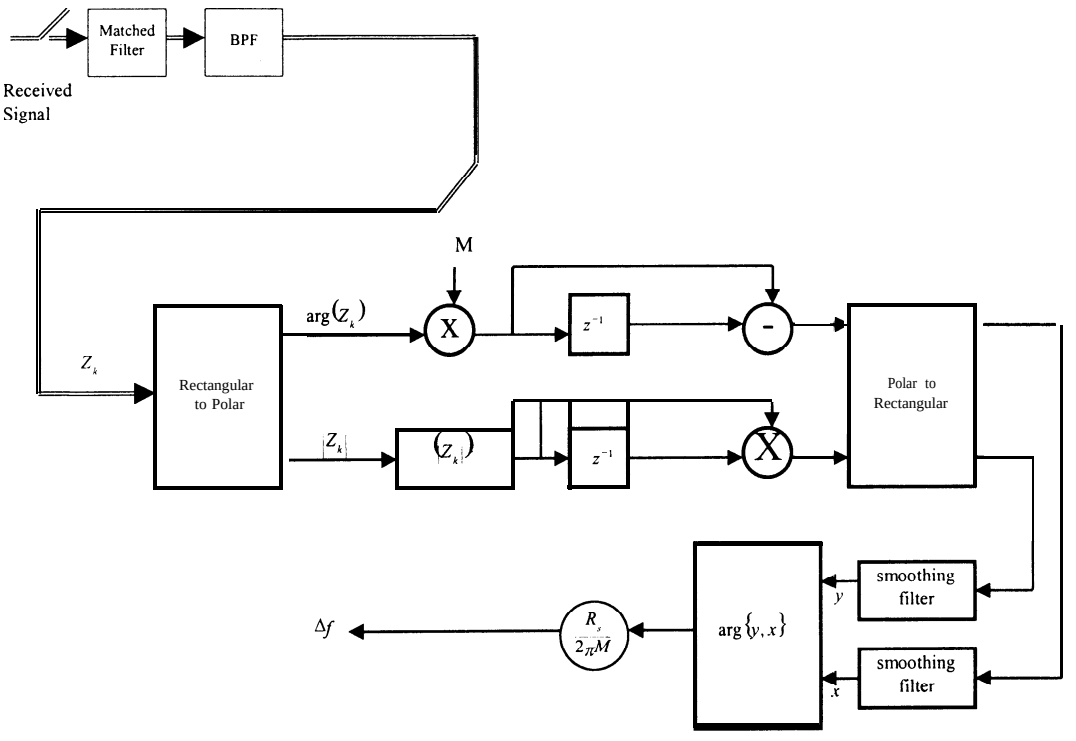

Figure 5: Viterbi carrier offset estimator algorithm

11.2. Viterbi Frequency Acquisition Algorithm

Another form of the M[th] power algorithm was developed by Viterbi [6]. This algorithm employes two separate non-linearity operators, one operates on the argument A4 arg(&-hl ;, and one operates on the magnitude of the Matched filter output $\left(\left|z_k z_{k-N}^*\right|\right)^\ell$. This algorithm have been proven to yield better performance for some particular modulations for low signal to noise ratios (especially for QAM modulations [6]). The Viterbi frequency offset estimates is defined by (10)

$$\Delta\hat{f} = \frac{R_s}{2\pi M}\arg\left\{\sum_0^{L-1} d_m\left(\left|z_k z_{k-N}^*\right|\right)^\ell e^{jM\left(\arg(z_k z_{k-N}^*)\right)}\right\} \quad (10)$$

where d, is a smoothing filter designed to provide robustness when operating at low SNR and to counteract slow signal variations that may be present due to multi-path attenuation. Figure 5 shows an implementation of this algorithrn. The smoothing filter can be a simple single low pass filter with a digital transfer function given by d_m- -[1] 1-p-l -, where p is a constant such that 0 < p < 1.

II.3. Symbol Correlation Based Acquisition Algorithm

Although simpler to implement, the M[th] power and Viterbi algorithms presented above suffer from self-noise generated by the use of the non-linearity process for removing data modulations. For QPSK, the use of the 4[th] order non-linearity results in a 6-dB rise of noise floor, and 3 dB of noise increase for the BPSK signals. Several other algorithms have been employed which are based on the sample to sample correlation function and do not use non-linearity processing. These algorithms involve more computational complexity. The complexity comes from the fact that it takes $N(2L-N-1)/2$ complex multiplications to perform the auto-correlation of two consecutive complex samples of the matched filter. One such algorithm was developed by Luise and Reggiannini in [14]. The frequency-offset estimations is given by (11)

$$\Delta\hat{f} = \frac{R_s}{2\pi}\sum_{k=1}^{N} w(k)[\arg R(k) - \arg R(k-1)] \qquad (11)$$

where the window function is given by

$$w(k) = \frac{3[(L-k)(L-k+1) - N(L-N))]}{N(4N^2 - 6NL + 3L^2 - 1)}$$

and the symbol correlation function given by

$$R(k) = \frac{1}{L-j}\sum_{k=j}^{L-1} z(k)z^*(k-j)$$

where $1 \le j \le N$, $N \le L/2$. The algorithm's capture range is given by $\Delta f = 2R_s/10$ Hz, which is comparable to the Viterbi and the M^{th} power algorithms.

Kay introduced a similar version to this algorithm, where the frequency estimates is given by (12)

$$\Delta\hat{f} = \frac{R_s}{2\pi}\sum_{k=1}^{N} w(k)\arg\{z(k)z^*(k-1)\} \qquad (12)$$

with the window function given by

$$w(n) = \frac{6k}{N(N+1)(2N+1)}$$

Luise&W [10] introduced another form of this algorithm, where the frequency estimate is given by (13)

$$\Delta\hat{f} = \frac{R_s}{2\pi}\arg\left\{\sum_{k=0}^{N-1} w(k)e^{j\arg\{z(k)\} - j\arg\{z(k-1)\}}\right\} \qquad (13)$$

Where the window function (parabolic) is given by

$$w(k) = \frac{6k(L-k)}{L(L^2-1)}.$$

L&W's capture range is $\Delta f = R_s/10$ Hz.

Fitz introduced another version in [10], with frequency estimation is given by (14)

$$\Delta\hat{f} = \frac{2R_s}{\pi N(N+1)} \sum_{k=1}^{N} \arg\{R(k)\} \quad (14)$$

with a capture range of $\Delta f = R_s/2N$ Hz.

Finally, L&R introduced another version that is similar to (12), where the frequency estimate is given by (15)

$$\Delta\hat{f} = \frac{R_s}{\pi(N+1)} \arg\left\{\sum_{k=1}^{N} R(k)\right\} \quad (15)$$

with a capture range of $\Delta f = R_s/N$ [Hz].

Mengali and Morelli reported simulation [10], which showed that these algorithms have the same performance for SNR more than 14 dB for QPSK modulations. However, with different capture ranges as indicated above.

II.4. DFT-Based Acquisition Algorithm

Another technique for estimating the frequency offset is based on DFT [9]. Unlike the algorithms discussed before; this algorithm does not require symbol-timing estimates. Figure 6 shows the digital implementation of this algorithm. The frequency-offset estimate is by (16)

$$\Delta f = \frac{R_s}{4\pi} \arg\left(\sum_{k=0}^{k=L} [C_{-1}(k) C_{+1}(k)]\right) \text{ [Hz]} \quad (16)$$

where $C_{-1}(k) = \sum_{L} z(k) z^*(k-N) e^{j\frac{2\pi n}{N}}$, and $C_{+1}(k) = \sum_{L} z(k) z^*(k-N) e^{j\frac{-2\pi n}{N}}$

Notice that $C_{-1}(k)$ and $C_{+1}(k)$ are conjugate pairs, this helps in saving computational resources on the DSP chip. This algorithm has a maximum capture range of $\Delta f \le \frac{R_s}{N}$ Hz, where N is the number of samples per symbols. We have found [10] that this algorithm does not yield acceptable performance, unless the matched filter signal has been filtered using a bandpass filter. The filter bandwidth varies depending on the roll off factor (α)

used. The filter should be designed with center frequency at the spectral component of interest in $z(kT)$, which contribute to the periodic component of interest in $z^*((k-N)T)z(kT)$. Roughly, the BPF should have a center frequency of $R_s/2$ Hz, and a bandwidth that is equal to αR_s.

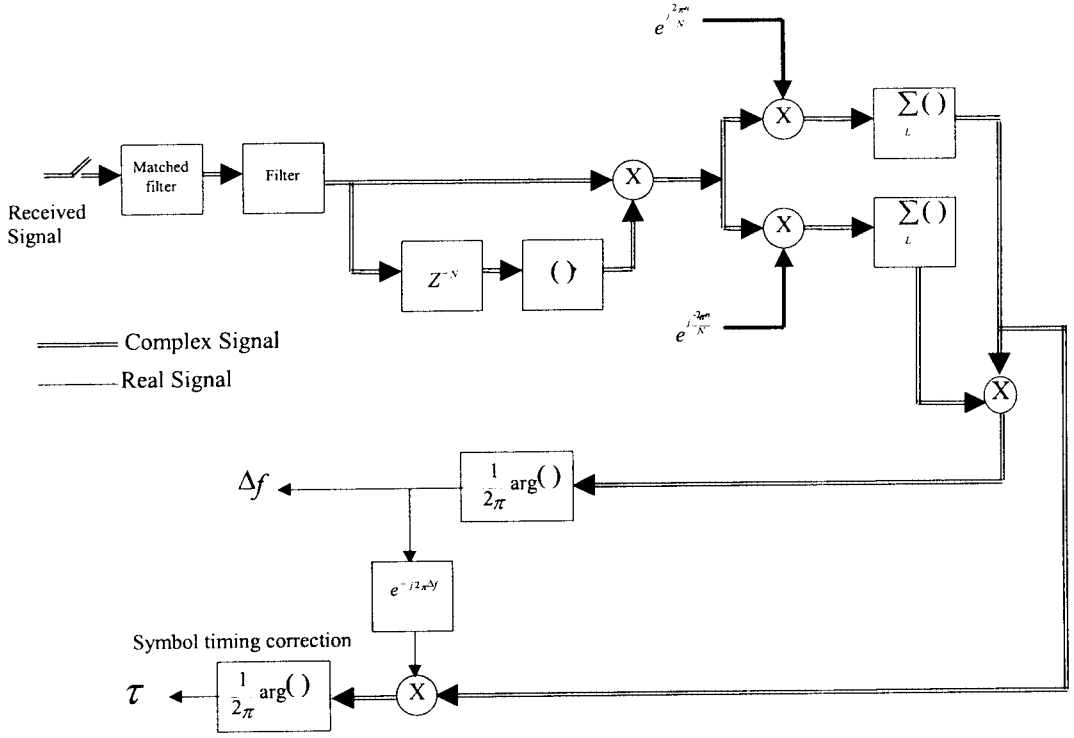

Figure 6: Joint symbol timing and carrier offset estimation algorithm using DFT

III. Conclusion

feedback and feed forward techniques were presented for carrier frequency acquisition. Tradeoffs between these algorithms were introduced in term of their implementation complexity, their estimation accuracy, and their frequency capture range. Computer simulations were used to show their performance in AWGN channels for QPSK modulations.

Acknowledgment

The author would like to acknowledge Dr. Sudhakar of Florida Atlantic University, Dr. Bard and Mr. H. Weeter of Mnemonics Inc. for contributing to this work.

Bibliography

The author hold BSEE and MSEE from University of Colorado. Currently he is a Ph.D. candidate at Florida Atlantic university and principle design engineer at Mnemonics inc., Florida. He can be reached at 321-253-7300 or E-mail mohamed_nezami@hotmial.com.

References

1. J. Bard, M. Nezami, and M Diaz "Data Recovery in Differentially Encoded Quadrature Phase Shift keying", Milcom2000, Los Angeles, CA., Ott 2000.

2. J. M. Nezami and Bard, " Preamble-less carrier recovery in fading channels", Milcom2000, Los Angeles, CA, Ott 2000.

3. M. Nezami and R. Sudhakar, "New schemes for 16-QAM symbol recovery", EUROCOMM 2000 Munich, Germany 17-l 9 May 2000

4. M. Nezami and R. Sudhakar, " M-QAM digital symbol timing synchronization in flat Rayleigh fading channels", PRMIC, Osaka Japan, Nov-1999.

5. M. Nezami, "DSP algorithms for carrier offset estimation and correction" ICSPAT, Orlando, Florida, USA, November-l 999.

6. M. Nezami and H. Otum, "Fine tuning frequency offset errors in M-QAM digital burst receivers using DSP techniques", Third international conference on computational aspects and their applications in electrical engineering, Amman, 19-20 October 1999.

7. M. Nezami, "Non-linear M-QAM digital symbol timing synchronization algorithm suited for wireless handheld radios". Third international conference on computational aspects and their applications in electrical engineering, Amman, 19-20 October 1999.

8. M. Nezami, "Digital synchronization algorithms for wireless burst QAM receivers", Wireless Symposium, San Jose, Ca/USA, Feb-1999.

9. M. Nezami, "An overview of DSP-based synchronization algorithms", Wireless Symposium, MA, USA-Sept- 1998.

10. Umberto Mengali and M. Moreli, "Data-Aided Frequency IEstimation for Burst Digital Transmission", IEEE trans. Communications, Vol. 45, Nao. 1, January 1997.